EXPERIMENTAL STUDY

Complete mid-portion rupture of the rat achilles tendon leads to remote and time-mismatched changes in uninjured regions

Flávio Santos da Silva[1] · Bento João Abreu[2] · Bengt I. Eriksson[3] · Paul W. Ackermann[4,5]

Abstract

Purpose To examine healing adaptations over 17 weeks post Achilles tendon (AT) rupture in the injured region (IR) compared to an uninjured region (UIR) of the AT.

Methods Twenty-four rats were subjected to a complete right-sided AT rupture, while the left side served as a control. ATs were harvested at 1, 2, 8 and 17 weeks post-rupture and stained with antibodies specific to Collagen type I (Col I) and II (Col II) as well as Alcian Blue and Picrosirius Red staining techniques. Histopathological changes, proteoglycan content, collagen alignment and immunoexpression were assessed.

Results Both regions examined, IR and UIR, exhibited over weeks 1–17 similar healing adaptations of increasing collagen alignment, decreasing Col I immunoexpression, as well as increasing proteoglycan content and Col II occurrence. Increased proteoglycan content was found already at week 2 in the UIR, while it first increased at week 8 in the IR. The area positive to Col II was increased compared to controls at week 8 in the UIR, whereas it first raised at week 17 in the IR. Collagen disorganization successively declined to reach control levels at week 17 in the UIR, but was still higher in the IR.

Conclusion This study demonstrated that uninjured areas of the AT remote from the rupture site also undergo pronounced remodeling, although with time-span differences relative to injured AT portions. These changes including the pathologic heterotopic mineralization and chondrogenic differentiation observed in both regions may have implications in the choice of rehabilitation regimes in order to prevent secondary rupture.

Keywords Tendon healing · Ossification · Chondrogenesis · Repair

✉ Paul W. Ackermann
  paul.ackermann@ki.se
  https://medarbetare.ki.se/people/pauack

  Flávio Santos da Silva
  flavionsp@gmail.com

  Bento João Abreu
  abreubj@gmail.com

  Bengt I. Eriksson
  bengt.eriksson@gu.se

1 Department of Health Sciences, Federal University of the Semiarid Region, Mossoró, Brazil

2 Department of Morphology, Federal University of Rio Grande do Norte, Natal, Brazil

3 Gothenburg University, Gothenburg, Sweden

4 Department of Molecular Medicine and Surgery, Karolinska Institutet, Stockholm, Sweden

5 Department of Orthopedic Surgery, Karolinska University Hospital, 17176 Stockholm, Sweden

Introduction

Tendons are soft and dynamic connective tissues responsible for transmitting muscle forces to bone in order to perform movement. The Achilles tendon (AT) is the largest tendon in the human body and it is able to withstand loads greater than 12 times the body weight [22]. However, the AT is also found among the most commonly injured tendons [16] and AT tendinopathies may cause considerable pain and disability [17].

After a complete AT rupture, the tendon structures lose their connection and the following healing process goes through three main overlapping stages [33]. In general, the initial phase spans over a few days and consists of formation of hematoma and a fibrin clot, as well as the recruitment of inflammatory cells to the injury site by chemotactic factors. Fibroblasts recruited to the wounded area start to secrete components of the extracellular matrix (ECM) during the inflammatory phase, but become more active during the

subsequent phase. In this proliferative phase, which lasts a few weeks, fibroblasts secrete proteoglycans, short-lived collagen types and other ECM components to build an immature scar. The remodeling phase starts after 6–8 weeks post-rupture and can continue for over one year. Remodeling is basically characterized by a decrease in cellularity, reduction of matrix production and a shift towards more stable type I collagen (Col I) synthesis and organization, which is associated with a progressive increase in the mechanical strength of the tissue.

The complete restoration of the AT after rupture is still a challenge for medicine. The failed tendon healing response may be present in the form of degeneration, random fibroblast proliferation, proteoglycan deposition, disruption of collagen organization and/or increase of the non-collagenous ECM [19]. Moreover, incidence of late mineralization in repaired human AT after injury may be as large as 14–62% [4] and mineralized areas may be a feature at the borders of injured tendons, next to the healing site [3]. However, it is not known whether these histopathological findings occur in a circumscribed manner at the injury site and whether regions remote from the injury site also exhibit comparable remodeling under a long period of tendon repair. This information may be useful for choosing appropriate rehabilitation regimes in order to prevent new episodes of tendon ruptures [8]. Thus, the aim of this study was to examine the presence of histopathological changes, proteoglycan content, collagen alignment and immunoexpression at the injury and a non-injured region of the AT in rats over a period of up to 17 weeks post-rupture.

Materials and methods

Animals and surgery procedure

Ethical approval was obtained from the Gothenburg Ethical Committee on Animal Research (Dnr. 257-2009). Briefly, the animals were housed and cared for at the Laboratory for Experimental Biomedicine (EBM, Gothenburg University). All animals were acclimatized and housed 3/cage for one week prior to surgical procedure. Tendon samples in this work were obtained from the same animals used elsewhere [27].

Twenty-four female Sprague–Dawley rats (40 days, ~200 g at the beginning of the experiment) were subjected to a complete rupture by tearing the middle-third of the right AT (Fig. 1) using an Ewald teeth forceps (TG instruments, Sweden). The rats were anesthetized via isoflurane inhalation (2–3%) and received pain medication (Temgesic, 0.3 mg/ml) pre- and post-surgery. The rupture was left unsutured while the skin over the lesion was closed with 2–3 nylon stitches. The left AT served as control. At the
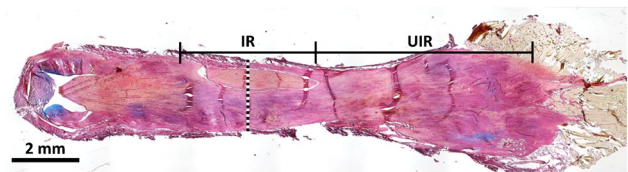

Fig. 1 Achilles tendon region definitions. *IR* injured region, *UIR* uninjured region. The location of surgical rupture is indicated by the dotted black and white line. ×100. Scale bar = 2 mm

end of the experiment (1, 2, 8 and 17 weeks post-rupture), the animals were euthanized in groups of 6/time-point by pentobarbital overdose (Apoteket production & Laboratorier AB, Sweden).

Tendon regions definition

Two regions, injury (IR) and proximal uninjured (UIR), were defined in both ruptured and non-ruptured control samples. The IR was set to a length of 4 mm beginning 5 mm from the tendon-calcaneal junction and the UIR was considered to be the rest of the tendon all the way up to the muscle–tendon junction (Fig. 1). The distal region was omitted in this study due to its common content of both chondrocyte-like cells and proteoglycans [27].

Histochemical processing and image acquisition

The AT complex from both right and left legs were dissected and immersed in Histofix solution (Histolab products AB, Sweden), decalcified in 0.5 M EDTA/0.5% paraformaldehyde solution (2 weeks), then washed, dehydrated and embedded in paraffin. Serial longitudinal sections (5 μm) from tendon samples were mounted on plus-slide glasses (Histolab products, Sweden) and used for histological and immunohistochemical staining as described in following sections. The same regions of interest of both IR and UIR regions were captured (100-fold magnification) and assessed by an examiner blinded to the study groups, time-points and tendon regions.

Quantitative detection of proteoglycans

Proteoglycan content in the tendon tissue was revealed by Alcian Blue/Hematoxylin/Van Gieson staining method. Photomicrographs from stained slides were saved as TIFF-files, coded and analyzed using ImageJ (1.49v; NIH, USA; https://rsb.info.nih.gov/nih-image/). Automated ImageJ functions including the Color Deconvolution plugin were implemented to separate Alcian Blue (AB) stain from the counterstains (Hematoxylin and Van Gieson) and measure

the AB-positive area, expressing it as a fraction of total stained area in each image [12].

Determination of fibrillar collagen organization

To measure changes in the spatial alignment of Picrosirius Red (PSR)-stained fibrillar collagen in brightfield images, the Fast Fourier Transform (FFT) algorithm was used in association with circular statistics [29]. Briefly, a custom-written ImageJ macro was applied to highlight fiber profiles and to obtain a radial sum of the FFT output for each image. Data representing the angular distribution of fibers were then used to calculate the circular standard deviation (CircSD) of each directional frequency distribution. The smaller the CircSD is, the more aligned are the fibers [31].

PSR-polarization microscopy was also used to assess collagen birefringence colors as they were demonstrated to vary with heterogeneity of fiber arrangement [15]. So, the hue component of the bright pixels in each image was segmented using ImageJ macros. Based on the hue frequency, ranges were defined for red, orange, yellow and green birefringence. The number of pixels within each hue range was measured and expressed as a percentage of the total number of bright pixels [2].

Immunohistochemistry staining

After paraffin removal and dehydration, a two-step antigen retrieval procedure was performed. First, both collagen I (Col I, 1/200, AB755P, Millipore, USA) and collagen II (Col II, 1/100, 2B1.5, Thermo Fisher, Rockford, USA) were treated with hyaluronidase (Sigma; 1 mg/ml in 1XPBS, pH 5.0) for 45 min at 37 °C, followed NaCl (10 mM, 20 min at 60 °C for Col I) or pepsin (Sigma; 1 mg/ml in TrisHCl, pH 2.0, 10 min at 37 °C for Col II) treatment. Washing and blocking steps were followed by incubation with primary antibodies at 4 °C overnight. The next day, one-hour incubation at room temperature with biotinylated secondary antibody (anti-rabbit for Col I and ant-mouse for Col II) was performed and followed by signal amplification using avidin–biotin-peroxidase reagent (Vectastain Elite ABC kit, Vector Laboratories, UK). To visualize the labeling, a liquid DAB-Substrate Chromogen system (DAKO, Carpinteria, USA) was used. Sections of rat spinal cord were used as Col I and II positive control and as negative control the primary antibody was substituted by buffer solution. Using ImageJ, separate defined thresholds of hue, saturation and brightness were obtained for image segmentation and calculation of fraction area (%).

Statistical analysis

Statistical calculations were performed with GraphPad Prism 7.0 (GraphPad Software, USA). Differences between groups over time were tested using mixed repeated-measure analysis of variance with Sidak post-hoc test. Group (control, ruptured) was defined as between-subject factor and time (weeks 1, 2, 8 and 17) as within-subject factor. Pearson correlations were conducted between measured parameters. The P value < 0.05 was considered significant.

Results

Proteoglycan content and collagen alignment

Figure 2a displays representative images of AB staining in the IR during 1, 2, 8 and 17 weeks after AT rupture in comparison to the control. In the remodeling healing periods (8 and 17 week post-rupture), areas of highly concentrated AB staining were observed in all ruptured tendons and quantification showed a significant increase of AB-positive areas at 8 weeks when compared to the control (Fig. 2b). At 17 weeks, however, the percentage of AB-positive areas was reduced to similar levels of weeks 1 and 2. In IR CircSD levels were significantly higher at all weeks as compared to controls (Fig. 2d). Between weeks 2 and 8, a significant decrease of CircSD levels was noticed in the ruptured tendons (Fig. 2d).

In the UIR, AB-positive areas were increased at 2 weeks in comparison with the control (Fig. 3a, b). The UIR also exhibited increased CircSD levels at 1, 2 and 8 weeks when compared to the control, but the CircSD levels significantly decreased between 2 and 8 weeks (Fig. 3b). The CircSD levels at 17 weeks were not statistically different when compared to the control (Fig. 3b).

Birefringence analysis

In the IR, the red pixels presented higher proportions at weeks 1, 2 and 17 and the orange pixels at all weeks, in comparison to the controls (Fig. 4a–c). Moreover, the fraction of red pixels in the IR significantly decreased at week 2 when compared to week 1. The fraction of pixels with yellow birefringence was increased in the IR in comparison with controls only at 17 weeks (Fig. 4d), while the proportion of green pixels was significantly lower at all weeks when compared to control tendons (Fig. 4e).

The UIR exhibited a similar pattern as observed in the IR for the orange, yellow and green pixels (Fig. 4h–j). The
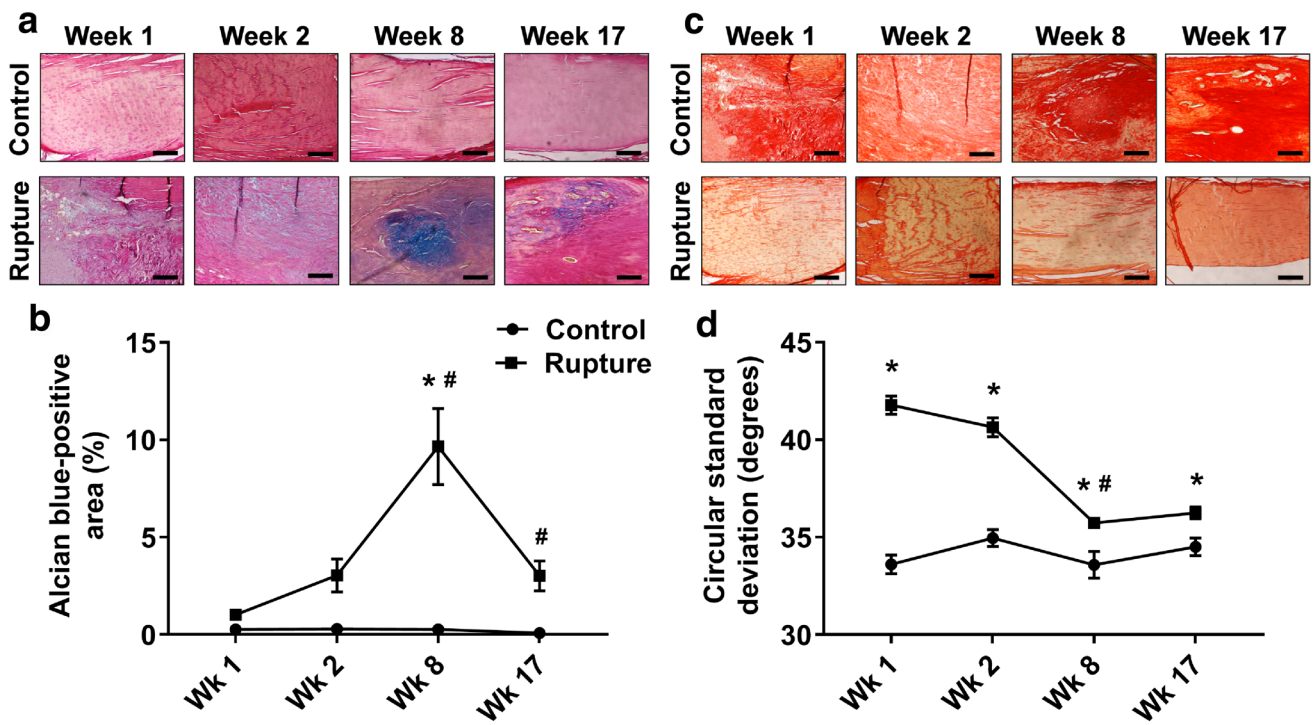
Fig. 2 Proteoglycan content (AB-positive area) (**a**, **b**) and collagen alignment (CircSD) (**c**, **d**) in the IR. *$P < 0.05$ vs. control; #$P < 0.05$ vs last week within rupture group. ×100. Scale bar = 100 µm
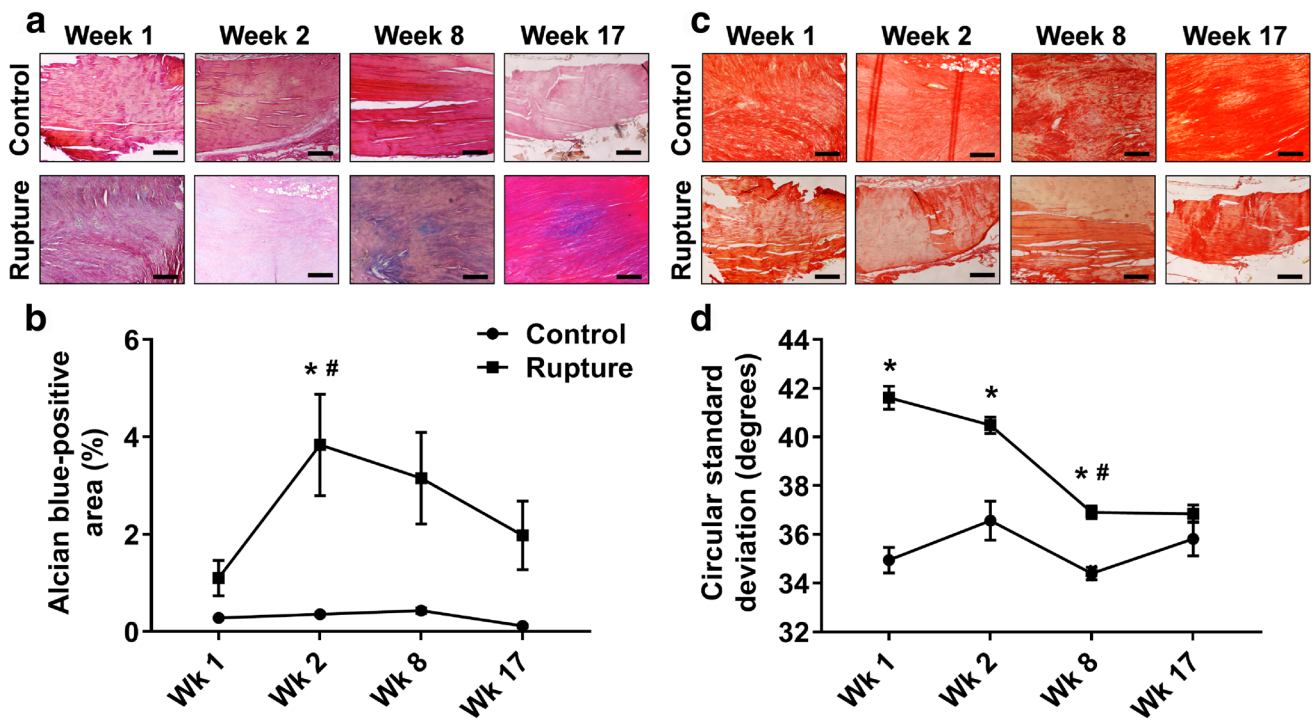

Fig. 3 Proteoglycan content (AB-positive area) (**a**, **b**) and collagen alignment (CircSD) (**c**, **d**) in the UIR. *$P < 0.05$ vs. control; #$P < 0.05$ vs last week within rupture group. ×100. Scale bar = 100 µm
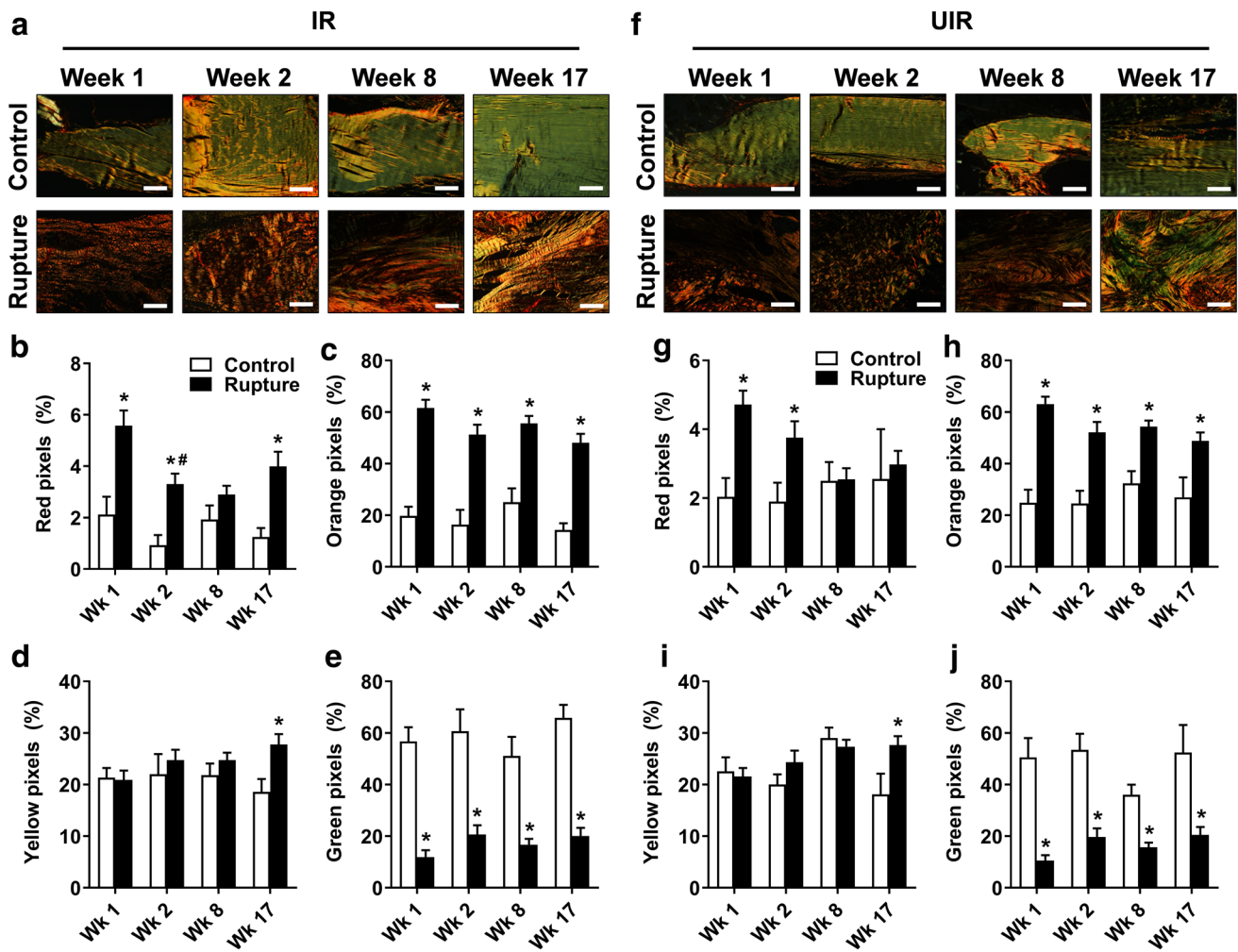
Fig. 4 Regional variation in collagen fiber hue over time in IR (**a**–**e**) and UIR (**f**–**j**) of the control and healing AT. The proportion of red and orange pixels decreased with time, while the proportion of yel-low and green pixels increased. *$P < 0.05$ vs. control at correspond-ing week. #$P < 0.05$ vs last week within rupture group. ×100. Scale bar = 100 µm

red pixel fraction in the UIR, however, was only increased at 1 and 2 weeks compared to controls (Fig. 4f–g).

Immunostaining of Col I and II

Areas positive to Col I in the IR were largely increased dur-ing all weeks of study in comparison with control (Fig. 5a, b). However, the percentage of areas immunostained for Col I declined significantly between weeks 2 and 8 and also con-tinued to drop between weeks 8 and 17 (Fig. 5b). Interest-ingly, the Col II positive areas in the IR started to increase from 8 weeks and presented significantly increased posi-tive immunostaining at 17 weeks when compared to control (Fig. 5c, d).

The UIR demonstrated a similar pattern of Col I positive areas as in the IR. However, the Col II positive areas in the

UIR were increased only at 8 weeks in comparison with control (Fig. 6).

Histopathological changes

While the control tendon showed no morphological altera-tions, the healing AT exhibited some alterations throughout its whole length during the remodeling phase. Foci of min-eralization were found in 3/6 of the rat ATs at 8 weeks post-injury, whereas at 17 weeks 5/6 of the tendons exhibited calcified tendon matrix. Figure 7 displays the histopathologi-cal features of a representative AT at week 17 post-rupture.

Pearson's correlation analyses

From week 2, an increasing number of significant corre-lations were observed up to week 17 in both IR and UIR
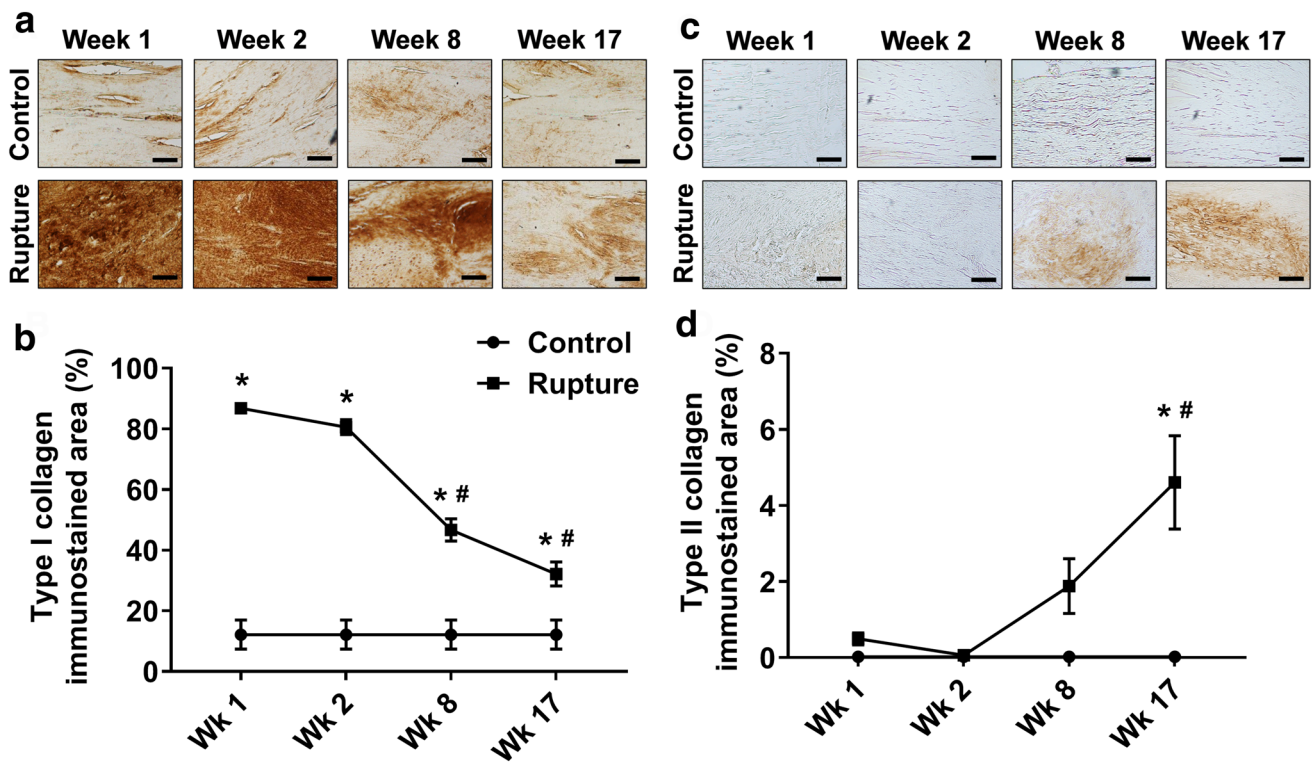
Fig. 5 Positive immunostaining area of Col I (**a**, **b**) and Col II (**c**, **d**) in the IR. *$P < 0.05$ vs. control; #$P < 0.05$ vs. last week within rupture group. ×100. Scale bar = 100 µm
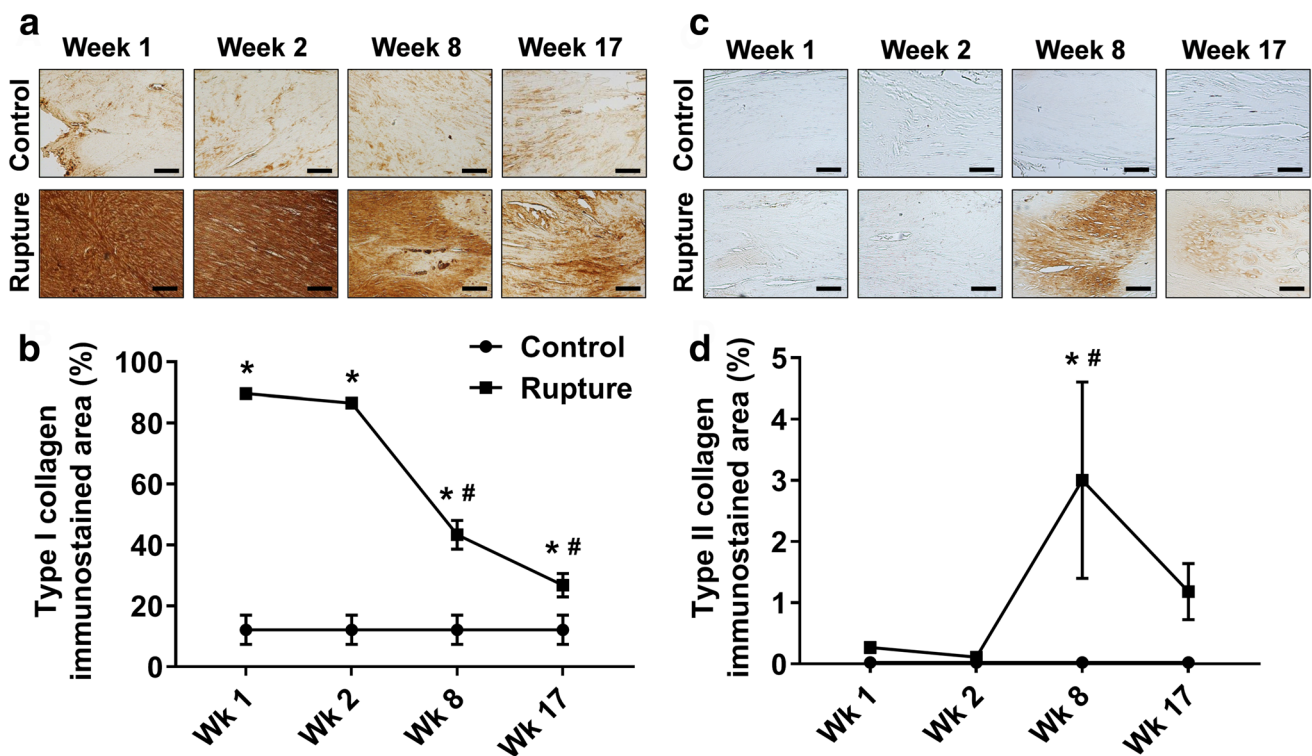

Fig. 6 Positive immunostaining area of Col I (**a**, **b**) and Col II (**c**, **d**) in the UIR. *$P < 0.05$ vs. control; #$P < 0.05$ vs. last week. ×100. Scale bar = 100 µm
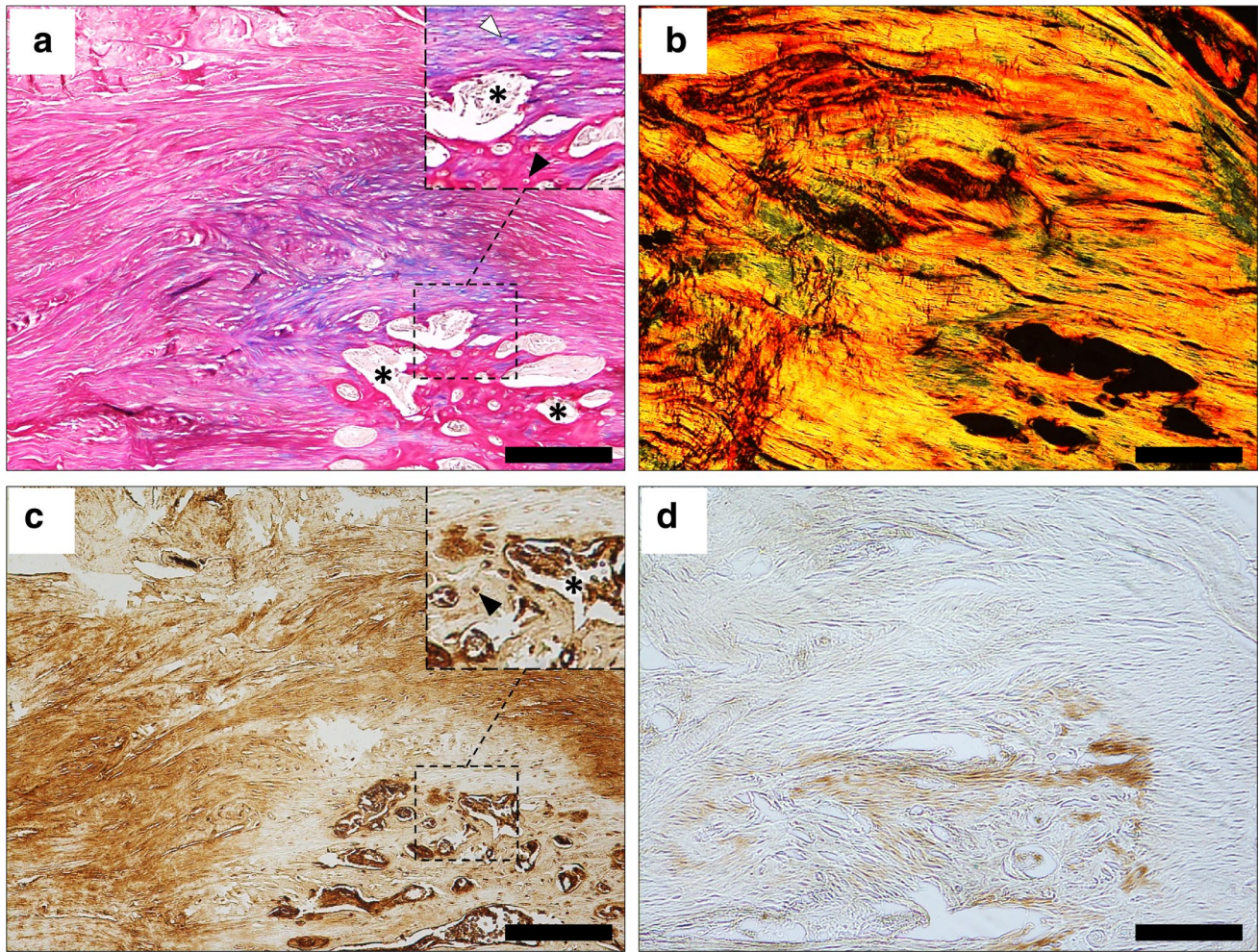
Fig. 7 Descriptive histology of a ruptured AT's UIR at 17 weeks. Higher magnification images show morphological alterations such as **a** cells presenting a round phenotype (white arrowhead) surrounded by chondroid islets (focal concentration of proteoglycans). Bone formation can also be recognized by areas of neovascularization (asterisks) next to round-shaped cells (black arrowhead) enclosed by an intense acidophilic material (mineralized ECM); **b** disposition of collagen fibers around the area of heterotopic ossification in a PSR-stained section viewed under polarized light; **c** Col I was immunolo-calized circumjacent to **d** Col II areas and within chondrocyte-like cells (black arrowhead). ×100 images. Scale bar = 100 μm

(Table 1). The strong and significant correlations ($r > 0.7$, $P < 0.05$) indicate that in the remodeling phase of healing the areas with poor collagen organization are linked to higher levels of both proteoglycans and Col II content (Table 1).

Discussion

The most important finding of the present study was that the UIR in addition to the IR undergo profound remodeling during long term tendon repair. However, both regions present temporal differences and distinct features regarding proteoglycan deposition, collagen alignment and expression. Notably, foci of mineralization and chondrogenic differentiation were observed in both regions studied.

To rule out that native tendons would exhibit changes in composition and microarchitecture over time, IR and UIR in control ATs were compared for proteoglycan content, CircSD, Col I and II protein expression. No statistical differences were found between regions (n.s.), reinforcing that changes in the ruptured ATs reflected diffuse ECM remodeling following surgical rupture.

In the late inflammatory and early proliferative phases, we found augmented reddish-orange hue proportions in the ruptured AT's IR and UIR, indicating that natural predominance of greenish-yellow birefringence (as seen in control ATs) were affected [15]. Moreover, the ruptured ATs presented high fractions of non-birefringent (dark) areas at the early repair. In brightfield examination, these areas spatially corresponded to an amorphous scar tissue. Initial accumulation

Table 1 Relationships among the studied variables over the experimental period in the IR and UIR

Time-points and variables	IR		UIR	
	r coefficient	P value	r coefficient	P value
Week 1				
AB vs CircSD	0.12	n.s	0.02	n.s
AB vs Col I	0.05	n.s	0.07	n.s
AB vs Col II	0.20	n.s	−0.12	n.s
CircSD vs Col I	0.26	n.s	−0.20	n.s
CircSD vs Col II	0.19	n.s	0.25	n.s
Col I vs Col II	0.11	n.s	−0.16	n.s
Week 2				
AB vs CircSD	0.12	n.s	−0.22	n.s
AB vs Col I	0.32	n.s	0.17	n.s
AB vs Col II	0.10	n.s	−0.18	n.s
CircSD vs Col I	0.29	n.s	−0.60	<0.01
CircSD vs Col II	−0.05	n.s	0.19	n.s
Col I vs Col II	0.16	n.s	0.13	n.s
Week 8				
AB vs CircSD	0.71	<0.01	−0.18	n.s
AB vs Col I	0.02	n.s	0.28	n.s
AB vs Col II	0.66	<0.01	0.84	<0.01
CircSD vs Col I	0.11	n.s	0.07	n.s
CircSD vs Col II	0.38	n.s	−0.13	n.s
Col I vs Col II	−0.09	n.s	0.47	<0.05
Week 17				
AB vs CircSD	0.46	<0.05	0.51	<0.05
AB vs Col I	0.52	<0.05	0.13	n.s
AB vs Col II	0.74	<0.01	0.67	<0.01
CircSD vs Col I	0.46	<0.05	0.34	n.s
CircSD vs Col II	0.58	<0.05	0.49	<0.05
Col I vs Col II	0.63	<0.01	0.16	n.s

Both regions exhibited correlations for AB vs Col II at week 8; and AB vs CircSD, AB vs Col II, and CircSD vs Col II at week 17

IR injured region, *UIR* uninjured region, *AB* Alcian Blue, *CircSD* circular standard deviation, *Col I* type I collagen, *Col II* type II collagen, *n.s.* non-significant

of this immature ECM might explain the almost lack of correlations in the first weeks. Yet, the UIR exhibited moderate increase of proteoglycan content already at week 2 and presence of Col I seemed to be related to better ECM arrangement (as shown by negative correlation between CircSD and Col I). The loose aspect of the newly formed scar tissue at early healing likely is associated with a relative unloading condition in the ruptured ATs. This in turn might have had a contributory role on adaptations involving Col I augmented synthesis and disorganization since it was more prominent at weeks 1 and 2 [14].

The areas immunopositive to Col I were augmented in both regions in the first weeks. Additionally, the levels of Col II were negligible in the early tendon healing phase.

Col II is non-tenocyte related gene involved in the formation of chondrogenic differentiation, heterotopic ossification and failed tendon healing, [20] being able to withstand compression and shear forces at the tendon/ligament-bone interface [28]. The absence of Col II in early healing is consistent with a previous study [10] and may thus indicates that the cells have not been transformed to a chondrogenic-like phenotype at this stage of healing. Together, these features are consistent with other studies demonstrating high levels of water, proteoglycan and matrix components in the early stages of tendon repair [25, 30].

Over the subsequent 8–17 weeks, collagen birefringence showed a tendency to gradually shift from reddish-orange towards a greenish-yellow control pattern in both regions of the ruptured AT, which coincided with the collagen becoming more aligned. In contrast to the UIR, which exhibited an early increase of proteoglycans already at 2 weeks, the amount of proteoglycan peaked at 8 weeks in the IR. At this 8-week time-point, a reduction of Col I and an increase of Col II immunoexpression was observed in both the IR and UIR. Col II was, however, expressed earlier in the UIR (8 weeks) than the IR (17 weeks) and a Col II-positive pericellular matrix was generally found circling chondrocyte-like cells.

It is possible that the bioactive molecules that are involved in promoting the cellular response during tendon repair [34] and the larger amount of a scar-like tissue in the IR may account for tendon healing differences between regions. In this way, it is noteworthy to mention that collagen alignment in the IR does not normalize during the 17 weeks period, whereas the UIR reaches alignment levels similar to those of the control. Collagen fiber disorientation during remodeling may result in a reduced tensile strength and predispose the tissue to tendinopathy [23]. In fact, complete healing restoration may take several months up to a year and tissue functional strength may not reach the levels of the healthy tendon [18].

Moreover, variations in collagen alignment may subject tendon tissue to different types (tensional, compressive and shearing) of loads, which may drive to diverse healing behavior. The observation that collagen orientation correlated positively with the content of both proteoglycans and of Col II at different time-points in the two regions supports the above conception. Thus, IR and UIR may experience different stimuli leading to chondrogenic differentiation and variation in ECM mineralization [9].

It is generally accepted that the formation of fibrocartilaginous tissue depends upon proteoglycan production in a stage prior to Col II formation [6, 24]. Interestingly, the UIR exhibited earlier proteoglycan and peak of Col II than the IR, suggesting that the chondrogenic/ossification processes begin in areas distant from the rupture site and reinforcing the observed time-span healing differences along the

AT. These areas of immature healing further resembles the histological features of heterotopic ossification, which have been previously reported in both tendinopathic and ruptured tendon from animals [1, 18, 20, 21, 35] as well as humans [6, 11]. Since imbalances within tendon may result in a tissue with sub-optimal structure and function [7], such abnormalities are believed to predispose the AT to spontaneous tear, and episodes of re-rupture may be common (up to 5% after surgical repair and up to 35% with non-operative treatment) [8]. Indeed, secondary tendon ruptures have been demonstrated outside initial rupture site in humans [26] and different tissue failure modes under tensile testing were observed in rats after complete mid-portion AT's rupture [5].

The cellular and molecular events involved in the formation of heterotopic ossification in tendons remain to be fully elucidated. Zhang et al. [35] reported ectopic tendon mineralization to be detected in injured mouse AT at week 8–10 post-surgery. They further found that mineralized tendon areas had increased at 25 weeks post-surgery, thus indicating the mineralization process to be progressive. However, their findings were observed only in the ruptured region and other tendon regions remote from the injury site were not evaluated. On the other hand, chondroid degeneration has been shown to be induced adjacent to injury through differentiation of specific progenitor cells [3].

Interestingly, our results showed that Col II was immunolocalized around chondrocyte-like cells in the immature islets, while Col I was expressed surrounding those islets and observed intracellularly. Since chondrocytes are able to co-express Col I and II depending on changes in their environment [32], tendon cell differentiation in the immature areas may be an attempt to recreate an environment for proper tendon reorganization. Thus, in pathological conditions as our rat AT injury model, the encircling pattern of the mature Col I structures on the proteoglycan and Col II-rich regions with disorganized stroma may constitute a border between areas with different mechanotransduction stimuli and responses to load.

This work has some limitations. First, the four healing time-points we select to study can not cover the whole course of the post-rupture AT micro-environmental internal changes. Another potential limitation of our study is the rat model of AT rupture, since rodents possess anatomical, kinematic and kinetic differences compared to humans [13] and then also the AT's healing responses.

Conclusion

This study provides evidence that AT portions remote from the rupture site also undergo profound remodeling, although time-span differences exist between regions during repair. Earlier proteoglycan deposition and more well-organized collagen alignment and Col II immunoexpression were observed in the UIR compared to the IR at the end of 17 weeks. Mineralization foci and chondrogenic differentiation were prominent features in both regions studied. These findings may have implications in the choice of rehabilitation regimes in order to prevent secondary tendon rupture.

Compliance with ethical standards

Conflict of interest The authors declare that they have no conflict of interests regarding the publication of this paper.

Ethical approval The Gothenburg Ethical Committee on Animal Research approved this study (Dnr. 257-2009).

References

1. Abraham T, Fong G, Scott A (2011) Second harmonic generation analysis of early Achilles tendinosis in response to in vivo mechanical loading. BMC Musculoskelet Disord 12:26
2. Aikawa E, Whittaker P, Farber M et al (2006) Human semilunar cardiac valve remodeling by activated cells from fetus to adult: implications for postnatal adaptation, pathology, and tissue engineering. Circulation 113:1344–1352
3. Asai S, Otsuru S, Candela ME, Enomoto-Iwamoto M et al (2014) Tendon progenitor cells in injured tendons have strong chondrogenic potential: the CD105-negative subpopulation induces chondrogenic degeneration. Stem Cells 32:3266–3277
4. Ateschrang A, Gratzer C, Weise K (2008) Incidence and effect of calcifications after open-augmented Achilles tendon repair. Arch Orthop Trauma Surg 128:1087–1092
5. Bring DK, Paulson K, Renstrom P et al (2012) Residual substance P levels after capsaicin treatment correlate with tendon repair. Wound Repair Regen 20:50–60
6. Burssens A, Forsyth R, Bongaerts W et al (2013) Arguments for an increasing differentiation towards fibrocartilaginous components in midportion Achilles tendinopathy. Knee Surg Sports Traumatol Arthrosc 21:1459–1467
7. Checa S, Rausch MK, Petersen A et al (2015) The emergence of extracellular matrix mechanics and cell traction forces as important regulators of cellular self-organization. Biomech Model Mechanobiol 14:1–13
8. Corradino B, Di Lorenzo S, Calamia C et al (2015) Surgical Repair Of Acute Achilles tendon rupture with an end-to-end tendon suture and tendon flap. Injury 46:1637–1640

9. de Mos M, Koevoet W, van Schie HT et al (2009) In vitro model to study chondrogenic differentiation in tendinopathy. Am J Sports Med 37:1214–1222

10. Dyment NA, Kazemi N, Aschbacher-Smith LE et al (2012) The relationships among spatiotemporal collagen gene expression, histology, and biomechanics following full-length injury in the murine patellar tendon. J Orthop Res 30:28–36

11. Erdogan F, Aydingoz O, Kesmezacar H et al (2004) Calcification of the patellar tendon after ACL reconstruction. A case report with long-term follow-up. Knee Surg Sports Traumatol Arthrosc 12:277–279

12. Finlay S, Seedhom BB, Carey DO et al (2016) In vitro engineering of high modulus cartilage-like constructs. Tissue Eng Part C Methods 22:382–397

13. Hast MW, Zuskov A, Soslowsky LJ (2014) The role of animal models in tendon research. Bone Jt Res 3:193–202

14. Khayyeri H, Blomgran P, Hammerman M et al (2017) Achilles tendon compositional and structural properties are altered after unloading by botox. Sci Rep 7:13067

15. Lattouf R, Younes R, Lutomski D et al (2014) Picrosirius red staining: a useful tool to appraise collagen networks in normal and pathological tissues. J Histochem Cytochem 62:751–758

16. Lemme NJ, Li NY, DeFroda SF et al (2018) Epidemiology of Achilles tendon ruptures in the United States: athletic and nonathletic injuries from 2012 to 2016. Orthop J Sports Med 6:2325967118808238

17. Li HY, Hua YH (2016) Achilles tendinopathy: current concepts about the basic science and clinical treatments. Biomed Res Int 2016:6492597

18. Lin TW, Cardenas L, Soslowsky LJ (2004) Biomechanics of tendon injury and repair. J Biomech 37(6):865–877

19. Longo UG, Ronga M, Maffulli N (2009) Achilles tendinopathy. Sports Med Arthrosc Rev 17:112–126

20. Lui PP, Chan LS, Lee YW et al (2010) Sustained expression of proteoglycans and collagen type III/type I ratio in a calcified tendinopathy model. Rheumatology (Oxford) 49:231–239

21. Lui PP, Fu SC, Chan LS et al (2009) Chondrocyte phenotype and ectopic ossification in collagenase-induced tendon degeneration. J Histochem Cytochem 57:91–100

22. Maffulli N (1999) Rupture of the Achilles tendon. J Bone Jt Surg Am 81:1019–1036

23. Magnusson SP, Langberg H, Kjaer M (2010) The pathogenesis of tendinopathy: balancing the response to loading. Nat Rev Rheumatol 6:262–268

24. Milz S, Benjamin M, Putz R (2005) Molecular parameters indicating adaptation to mechanical stress in fibrous connective tissue. Adv Anat Embryol Cell Biol 178:1–71

25. Müller SA, Todorov A, Heisterbach PE et al (2015) Tendon healing: an overview of physiology, biology, and pathology of tendon healing and systematic review of state of the art in tendon bioengineering. Knee Surg Sports Traumatol Arthrosc 23:2097–2105

26. Olaleye OA, Zahn H (2008) An unusual second rupture of the Achilles tendon: a case report. Foot Ankle J 1:3

27. Runesson E, Ackermann P, Karlsson J et al (2015) Nucleostemin- and Oct 3/4-positive stem/progenitor cells exhibit disparate anatomical and temporal expression during rat Achilles tendon healing. BMC Musculoskelet Disord 16:212

28. Sagarriga Visconti C, Kavalkovich K, Wu J et al (1996) Biochemical analysis of collagens at the ligament-bone interface reveals presence of cartilage-specific collagens. Arch Biochem Biophys 328:135–142

29. Schriefl AJ, Reinisch AJ, Sankaran S et al (2012) Quantitative assessment of collagen fibre orientations from two-dimensional images of soft biological tissues. J R Soc Interface 9:3081–3093

30. Sharma P, Maffulli N (2006) Biology of tendon injury: healing, modeling and remodeling. J Musculoskelet Neuronal Interact 6:181–190

31. Silva FS, Bortolin RH, Araújo DN et al (2017) Exercise training ameliorates matrix metalloproteinases 2 and 9 messenger RNA expression and mitigates adverse left ventricular remodeling in streptozotocin-induced diabetic rats. Cardiovasc Pathol 29:37–44

32. Tekari A, Luginbuehl R, Hofstetter W et al (2014) Chondrocytes expressing intracellular collagen type II enter the cell cycle and co-express collagen type I in monolayer culture. J Orthop Res 32:1503–1511

33. Voleti PB, Buckley MR, Soslowsky LJ (2012) Tendon healing: repair and regeneration. Annu Rev Biomed Eng 14:47–71

34. Yang G, Rothrauff BB, Tuan RS (2013) Tendon and ligament regeneration and repair: clinical relevance and developmental paradigm. Birth Defects Res C Embryo Today 99:203–222

35. Zhang C, Zhang Y, Zhong B et al (2016) SMAD7 prevents heterotopic ossification in a rat Achilles tendon injury model via regulation of endothelial-mesenchymal transition. FEBS J 283:1275–1285